Journal of Innovative Optical Health Sciences
Vol. 8, No. 5 (2015) 1550020 (10 pages)

DOI: 10.1142/S1793545815500200

World Scientific
www.worldscientific.com

A fast auto-focusing method of microscopic imaging based on an improved MCS algorithm

Guangkai Fu, Yiping Cao* and Mingteng Lu
Department of Optical Electronics
Sichuan University, Chengdu 610064, P. R. China
**ypcao@scu.edu.cn*

Received 17 September 2014
Accepted 23 November 2014
Published 24 December 2014

An improved "three steps" mountain-climb searching (MCS) algorithm is proposed which is applied to auto-focusing for microscopic imaging accurately and efficiently. By analyzing the performance of several evaluation functions, the variance function and the Brenner function are synthesized as a new evaluation function. In the first step, a self-adaptive step length which is much dependent on the reciprocal of the evaluation function value at the beginning position of climbing is used for approaching the halfway up the mountain roughly. Secondly, a fixed moderate step length is applied for approaching the mountaintop of the variance function as closer as possible. Finally, a fine step is employed for reaching the exact mountaintop of the Brenner function. The microscope auto-focusing experiments based on the proposed algorithm for blood smear detection have been carried out comprehensively. The results show that the improved algorithm can not only guarantee the precision to get clear focal images, but also improve the auto-focusing efficiency.

Keywords: Auto-focusing; evaluation function; mountain-climb searching algorithm; image processing.

1. Introduction

The microscope focusing technology which plays an important role in the image measurement and computer vision is widely used in biological and medical science.[1,2] However, microscope focusing to obtain image by manual operation has not meet the demand of precision, efficiency and instantaneity. The auto-focusing methods for microscope can be classified into the initiative controlling methods and image processing methods. In the initiative methods, the focused object must be plane and the plane must be perpendicular to the optical axis of the objective, so the object distance can be measured by additional equipment and focusing can be adjusted according to the measuring result initiatively. In the image processing methods, the focusing is adjusted by the clearness of the captured image in real-time,[3] so the evaluation function to judge the image clearness is the kernel of these methods.

*Corresponding author.

The auto-focusing based on image processing for microscope is achieved with image acquisition, computation of the image clearness and circuit feedback control. The image clearness is usually judged by some evaluation functions. So the key technologies of auto-focusing for microscope are evaluation function selection and focal plane searching algorithm. Recently, several evaluation functions have been developed such as variance function, Tenengrad function, energy gradient function, Brenner function and Entropy function.[4–9] An ideal evaluation function should have good performance of single-peak, unbiasedness and higher signal to noise ratio.[10,11] One of the focal plane searching algorithms is the mountain-climb searching (MCS) algorithm for its convenience to implement and easiness to control the amount of calculation.

The microscopic imaging detection for blood smear has been the most common and the most important technique for disease diagnosis. As is well known, the blood cells mainly consisted of erythrocyte, platelet and leukocyte.[12] The quantities, types and morphology of leukocyte are the main important features to reflect the health status. Generally, more than hundreds of clear 100× leukocyte images captured by microscope in a blood smear must be delivered for the doctor to diagnose the disease effectively. But the distribution of leukocyte is very sparse in a blood smear because the proportion of leukocyte is much smaller than that of erythrocyte in human peripheral blood. In order to capture sufficient 100× leukocyte images, hundreds of local regions must be scanned in the blood smear. Different defocus values at different local regions will be introduced because of the mechanical errors and motion errors of the object stage while scanning. Therefore, the real-time auto-focusing is indispensable and plays an important role to capture sufficient and clear 100× leukocyte images. So an improved "three steps" MCS algorithm is proposed to meet the above requirement of auto-focusing.

2. The Theory of MCS Algorithm

The basic MCS algorithm is as shown in Fig. 1. Firstly, the climbing direction must be judged by comparing the evaluation function values of the two images captured at C_0 and C_1, if the value at C_1 is bigger than that at C_0, the searching direction is just the climbing direction, otherwise the backward searching direction is the climbing direction. Then, we continually compare the evaluation function values of the current image and the last image captured at different positions while climbing until the current value is smaller than the last value which means the mountaintop has just been crossed. Finally, we search backward with smaller step length until we find the mountaintop.[13,14] In this way, the C_0-C_1-C_2-C_3-C_4-C_3 or C_1-C_0-C_1-C_2-C_3-C_4-C_3 climbing track has been left.

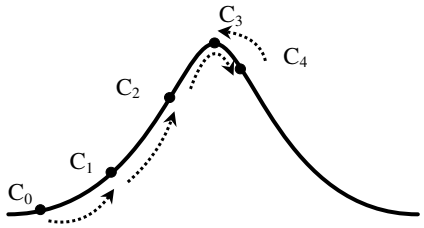

Fig. 1. The theory of the MCS algorithm.

This algorithm judges the searching direction by comparing two images evaluation function values which is relatively simple and easy to implement. But in practice, it may go astray from the global maximum (F_5) into the local maximum (F_2) due to the noises in the captured images as shown in Fig. 2. Song *et al.* proposed a global maximum searching algorithm by scanning the whole mountain in advance to mark the position of the rough global maximum and then approaching the real global maximum.[15] This method obviously will increase the searching time. Liqun *et al.* used the self-adaptive MCS algorithm that can adaptively adjust the searching range according to different environmental conditions.[16] Although this method can avoid the searching process falling into the local maximum, it will increase the search time as well.

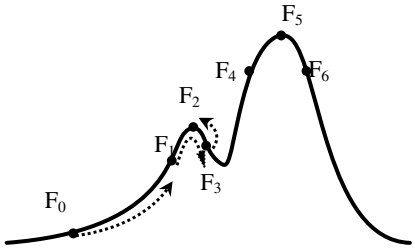

Fig. 2. The circumstances of false MCS.

3. The Improved "Three Steps" MCS Algorithm

In the microscopic imaging detection for blood smear, the distribution of leukocyte is sparse in a blood smear because the proportion of leukocyte is much smaller than that of erythrocyte in human peripheral blood. Figure 3 shows a captured image under 10× objective in which only two pieces of leukocyte (L_1 and L_2) are mingled in the thousands of erythrocyte. In order to extract sufficient and clear region of interest (ROI) leukocyte images in every blood smear under 100× objective, the auto-focusing must be operated frequently at different scanned local regions because of the limited smaller view field of CCD camera. So the real-time performance plays a most important role in this circumstance. The improved "three steps" MCS algorithm can meet this auto-focusing requirement.

3.1. *The evaluation function*

In order to find a proper evaluation function to achieve fast auto-focusing for microscopic leukocyte imaging, five evaluation functions are analyzed comprehensively. For a captured image I, the variance function F_{var}, the Tenengrad function F_{Ten}, the energy gradient function F_{Ene}, the Brenner function F_{Bre} and the Entropy function F_{Ent} can be described by Eqs. (1)–(5) respectively:

$$\begin{cases} u = \dfrac{1}{MN}\displaystyle\sum_{x=1}^{M}\sum_{y=1}^{N} I(x,y) \\ F_{\text{var}}(I) = \displaystyle\sum_{x=1}^{M}\sum_{y=1}^{N}[I(x,y)-u]^2 \end{cases}, \tag{1}$$

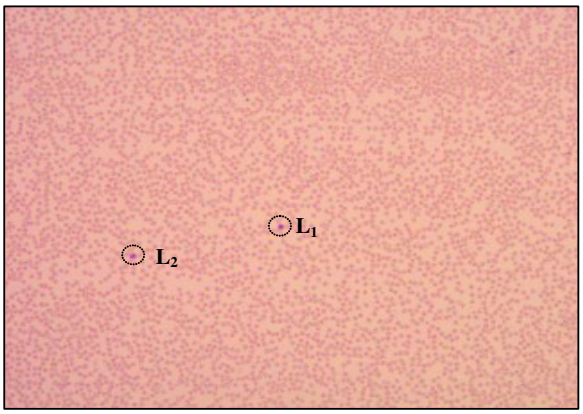

Fig. 3. One of the captured images in a blood smear under 10× objective.

$$\begin{cases} G_x(x,y) = I(x-1,y+1)+2I(x,y+1) \\ \qquad +I(x+1,y+1)-I(x-1,y-1) \\ \qquad -2I(x,y-1)-I(x+1,y-1) \\ G_y(x,y) = I(x-1,y-1)+2I(x-1,y) \\ \qquad +I(x-1,y+1)-I(x+1,y-1) \\ \qquad -2I(x+1,y)-I(x+1,y+1) \\ S(x,y) = \sqrt{G_x^2(x,y)+G_y^2(x,y)} \\ F_{\text{Ten}}(I) = \displaystyle\sum_{x=1}^{M}\sum_{y=1}^{N}[S(x,y)]^2 \end{cases}, \tag{2}$$

$$F_{\text{Ene}}(I) = \sum_{x=1}^{M}\sum_{y=1}^{N}\{[I(x+1,y)-I(x,y)]^2 + [I(x,y+1)-I(x,y)]^2\}, \tag{3}$$

$$F_{\text{Bre}}(I) = \sum_{x=1}^{M}\sum_{y=1}^{N}[I(x+2,y)-I(x,y)]^2, \tag{4}$$

$$F_{\text{Ent}}(I) = -\sum_{x=1}^{M}\sum_{y=1}^{N} I(x,y)\ln[I(x,y)], \tag{5}$$

where the $I(x,y)$ is the gray level intensity of pixel (x,y) of the image, u represents the average gray value of the image, N is the total lines and M is the total pixels per line of the image. Although the values of the above five evaluation functions are much different at the same defocus position, by normalization, they can be compared in the same condition. Figure 4 shows the normalized curves of the above five evaluation functions. Figure 4(a) reveals the curve tendencies under the 10× objective and so does the Fig. 4(b) under the 100× objective. By analyzing Fig. 4, some important information can be extracted: Firstly, all the five evaluation function curves have the same global maximum which is corresponding to the focal plane though their tendencies are somehow different. Secondly, Fig. 5 shows the zoom in of A and B regions in Fig. 4, it reveals that some local maximums exist under the halfway of each mountain of the above five evaluation function curves objectively caused by some noises. Thirdly, the tendencies of Tenengrad function, the energy gradient function and the Brenner function are similar with higher sensitivity and narrower region which cannot be used directly in the blood smear detection auto-focusing for the wider defocus region caused by the mechanical errors and motion errors of the object stage while scanning. But the tendencies of the variance function and the Entropy function are similar with wider

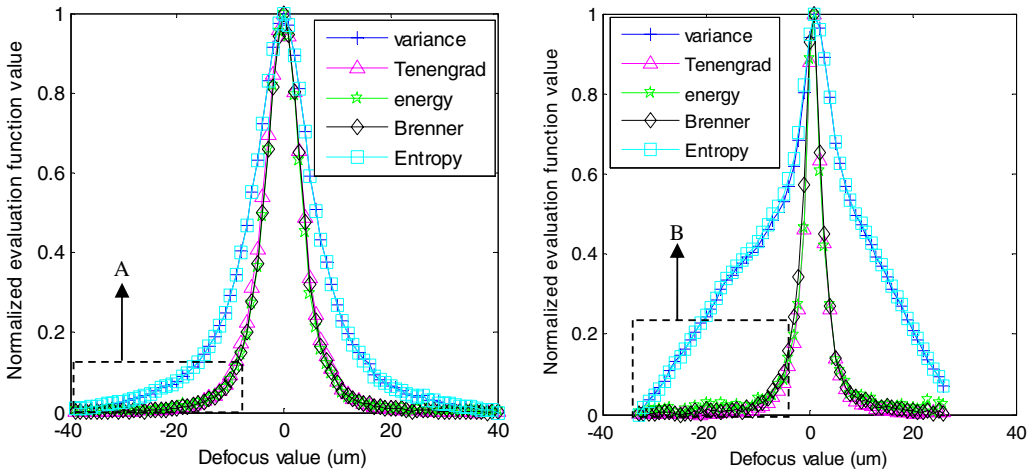

Fig. 4. Five normalized evaluation functions with different objectives. (a) The normalized curves under 10× objective and (b) the normalize curves under 100× objective.

region though with a little bit lower sensitivity. So if a new evaluation function can inherit the higher sensitivity performance of the former three evaluation functions and the wider region performance of the later two evaluation functions, it may suitable to meet the requirements of blood smear detection auto-focusing with wide region and high sensitivity. In order to improve the searching speed, many time consumption experiments of each of the above evaluation function for auto-focusing have been done. Table 1 shows the average time consumption ($\bar{t}$) of the above five evaluation functions, the where the $\bar{t}$ of variance function is much shorter than that of Entropy function, and the $\bar{t}$ of Brenner function is the shortest among those of Tenengrad function, the energy gradient function and the Brenner function. Therefore, a new evaluation function synthesized by variance function and Brenner function has been established in which the variance function is selected for a rough mountaintop searching in wide region and the Brenner function is selected for the real mountaintop searching in narrow region.

3.2. *The selection of step length and the algorithm implementation*

In order to search the real mountaintop as fast as possible, appropriate climbing step length selection is very important. Too big step length will lead to low accurate mountaintop searching or even failing the mountaintop searching; too small step length may lead to slow mountaintop searching or even

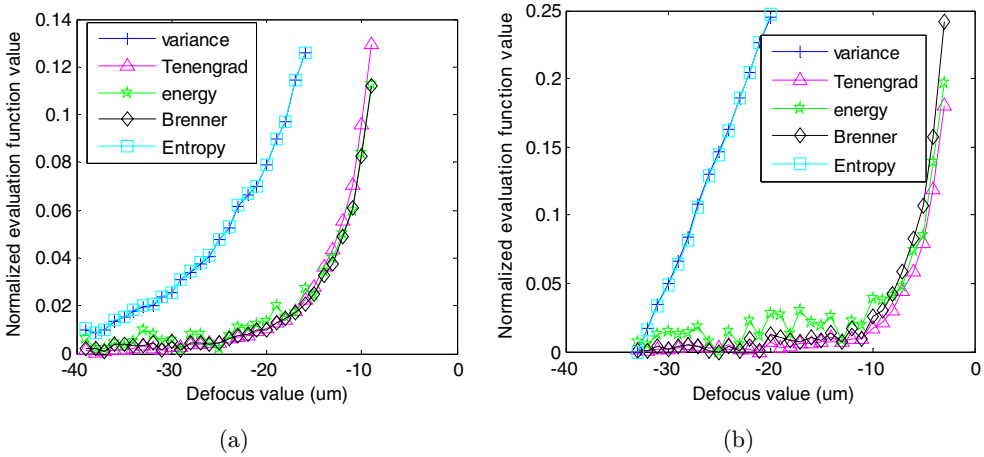

Fig. 5. The zoom in of different regions in Fig. 4. (a) The zoom in of A region and (b) The zoom in of B region.

Table 1. The average time consumption at different evaluation functions (ms).

Functions	Variance	Tenengrad	Energy gradient	Brenner	Entropy
$\bar{t}$	3.09	20.25	3.77	1.47	11.44

falling into the region with some local maximums depending on the beginning position of climbing. As analyzed above, the local maximums are located under the halfway of mountain, so skipping these local maximums is a very important gist. If a step length ($step_1$) while taking the first step is self-adaptively variable, it may avoid falling into the region with some local maximums. The variable $step_1$ must meet the requirements as follows: Firstly, it is much depended on the beginning position of climbing. The farther away it is from the mountaintop, the bigger it is and vice versa. Secondly, it must guarantee that the rough mountaintop searching would skip the local maximums and begin at the nearer mountaintop as possible as it can. Thirdly, it must be indeed used as judging the effective climbing direction. Having summarized from lots of experiments, it is found that the $step_1$ is inversely proportional to the value of variance function $F_{\text{var}}(I_0)$ by capturing the image I_0 at the beginning position of searching as follows:

$$step_1 = round\,(k/F_{\text{var}}(I_0)), \tag{6}$$

where the $round()$ is round-off operator and the k is a proper proportion coefficient which is much depended on the focused object. Different focused objects may lead to a little bit change for k. In the microscopic imaging detection for blood smear, there are five typical types of leukocyte such as neutrophil (Neu), lymphocyte (Lym), monocyte (Mon), eosinophil (Eos) and basophil (Bas)[17,18] as shown in Fig. 6. The extracted fives types of leukocyte images from different ROI in a blood smear are analyzed with the variance function. Figure 7(a) shows that the variance functions for the five types of leukocyte images

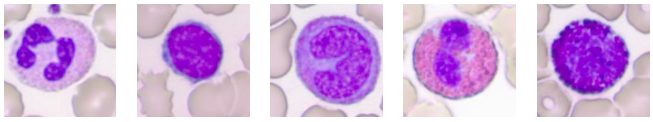

(a) (b) (c) (d) (e)

Fig. 6. The five types of ROI leukocyte images. (a) Neu, (b) Lym, (c) Mon, (d) Eos and (e) Bas.

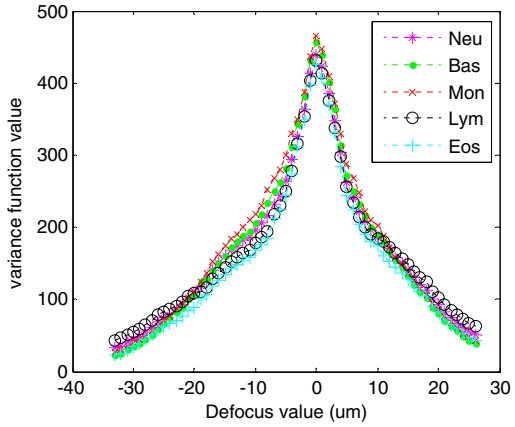

(a)

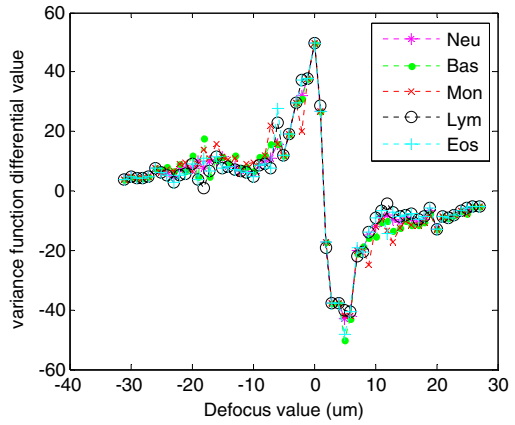

(b)

Fig. 7. The variance function and its differential at different ROI. (a) The variance function and (b) The differential of the variance function.

have the similar tendencies though their values are different at the same defocus positions, Fig. 7(b) shows the differential of these variance functions, in Fig. 7(a), it reveals that the five differential curves nearly overlap and the function values change sharply when the defocus range is from -8 um to 8 um which means that it is nearly approaching the mountaintop of the curve, so by analyzing the specific data in Fig. 7(a), the k value range should be from 1500 to 1700.

By analyzing above, the improved "three steps" of the MCS algorithm can be highlighted: Firstly, a self-adaptive step length ($step_1$) is much dependent on the reciprocal of the evaluation function value at the beginning position of climbing and is used for approaching the halfway mark of the mountain roughly. Secondly, a fixed moderate step length ($step_2$) is applied for approaching the mountaintop

of the variance function as closer as possible in the coarse focusing. Finally, a fine step ($step_3$) is employed for reaching the exact mountaintop of the Brenner function in the fine focusing.

The fast auto-focusing process flow chart for the leukocyte images with the improved "three steps" MCS algorithm is as shown in Fig. 8. Firstly, it calculates $F_{\text{var}}(I_0)$ by capturing the image I_0 at the beginning position of searching with Eq. (1) and the self-adaptive $step_1$ with Eq. (6). Then it takes a step with $step_1$ and calculates $F_{\text{var}}(I_i)$ by capturing the image I_i at current position. If $F_{\text{var}}(I_i)$ is bigger than $F_{\text{var}}(I_0)$, the searching direction is just the climbing direction and the current position is definitely up the halfway of mountaintop; otherwise the searching direction must be changed backward and the current position may be located up or down the halfway of the mountain or evenfall into the region with some local maximums. So a moderate value ΔF_0 is introduced to judge whether the current

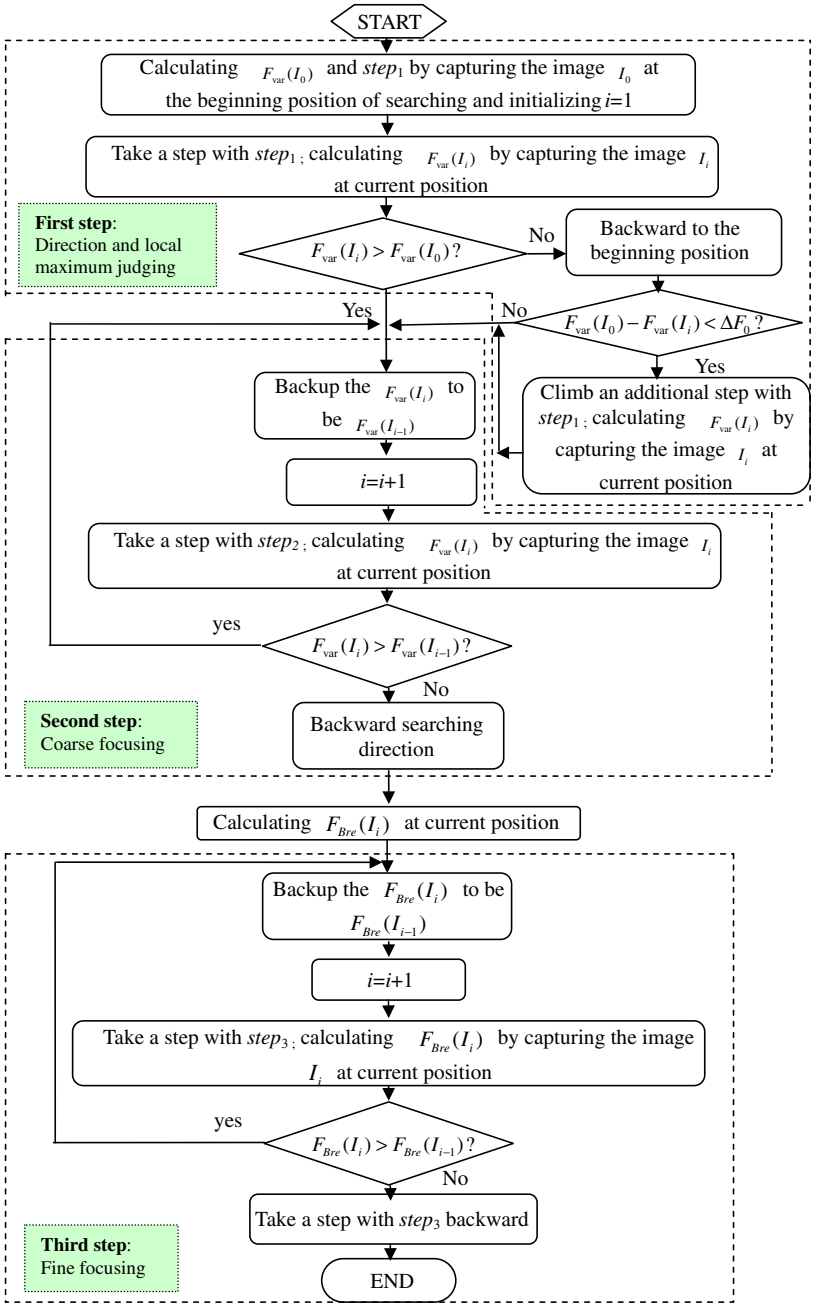

Fig. 8. The auto-focusing flow chart.

position is falling into the region with some local maximums or not and it is also much depended on the focused object. By analyzing the specific data in Fig. 7(a), ΔF_0 should be 75. So $F_{\text{var}}(I_0) - F_{\text{var}}(I_i) < \Delta F_0$ reveals that the current position has fallen into the region with some local maximums. If it takes an additional step along the climbing direction with double $step_1$, the current position is also definitely up the halfway of the mountain. In this way, the current position has been up the halfway of the mountain by taking only one or two steps; Then the current $F_{\text{var}}(I_i)$ is backed up to be the last $F_{\text{var}}(I_{i-1})$ and it takes a step with $step_2$ and calculates the current $F_{\text{var}}(I_i)$, by continually comparing the current $F_{\text{var}}(I_i)$ and the last $F_{\text{var}}(I_{i-1})$ repeatedly until $F_{\text{var}}(I_i) < F_{\text{var}}(I_{i-1})$. In this way, the rough mountaintop has been found as the last position; in the same way by substituting $step_3$ for $step_2$ and substituting $F_{\text{Bre}}(I_i)$ for $F_{\text{var}}(I_i)$, the real mountaintop can finally be found accurately.

4. Experiment and Analysis

In order to verify the feasibility and validity of the improved MCS algorithm, lots of auto-focusing experiments based on the improved MCS algorithm under different magnification objectives have been carried out in the microscopic imaging detection for blood smear.

The experimental system is shown in Fig. 9, an improved OLYMPUS BX53 microscope which can realize auto-capturing leukocyte image with a MD55 camera, auto-focusing by driving the electric controlled object stage up and down and auto-scanning

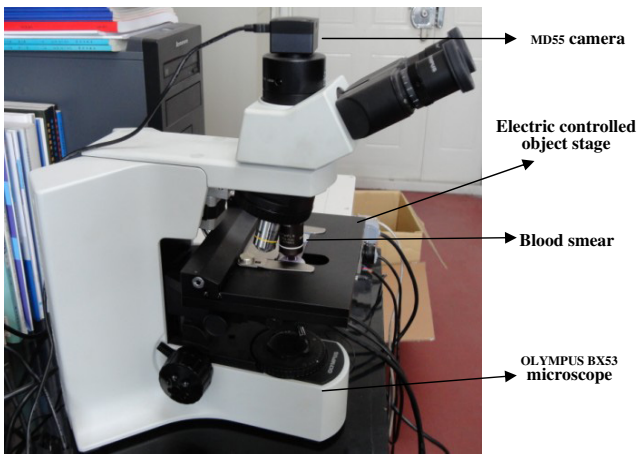

Fig. 9. The auto-focusing system experimental device.

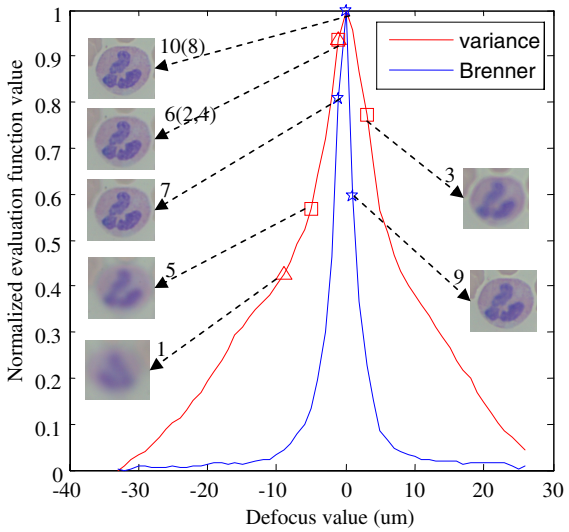

Fig. 10. The auto-focusing process at the beginning position of negative defocus near the focal plane.

by driving the electric controlled object stage rightward and leftward or forward and backward with a three-axis step motor controlling system.

Figures 10–13 have revealed the auto-focusing processes in detail at different beginning defocus positions in which the triangle symbols, the rectangle symbols and the pentagon symbols present the three steps of the "three step" MCS algorithm, respectively.

There are four possible beginning position circumstances in the auto-focusing. Firstly, the beginning position is near the focal plane with negative defocus. Figure 10 shows one of the experimental

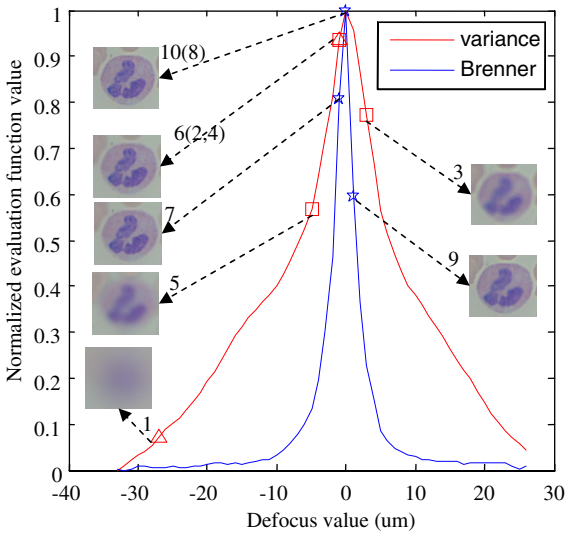

Fig. 11. The auto-focusing process at the beginning position of negative defocus far from the focal plane.

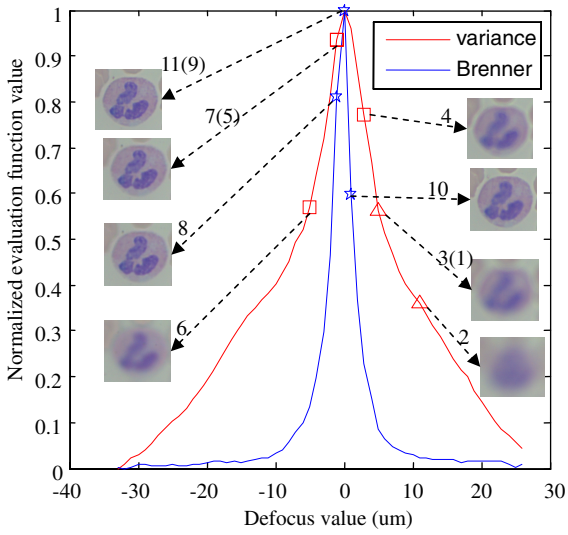

Fig. 12. The auto-focusing process at the beginning position of positive near the focal plane.

results under this circumstance. The beginning position is −9 um near the focal plane. The $F_{\text{var}}(I_0)$ is calculated with Eq. (1) to be 205.96 as shown in the variance function of Neu images in Fig. 7(a), then the self-adaptive $step_1$ will be figured out to be 8 um with Eq. (6). By taking a step with $step_1$, the current position comes to −1 um near the focal plane which means it is definitely up the halfway of the mountain and away from the region with many local maximums. While the $step_2$ is fixed as 4 um, it takes only four steps to finish searching the rough mountaintop. While changing $step_2$ to be $step_3$ with 1 um, it takes only the other three steps to reach the real

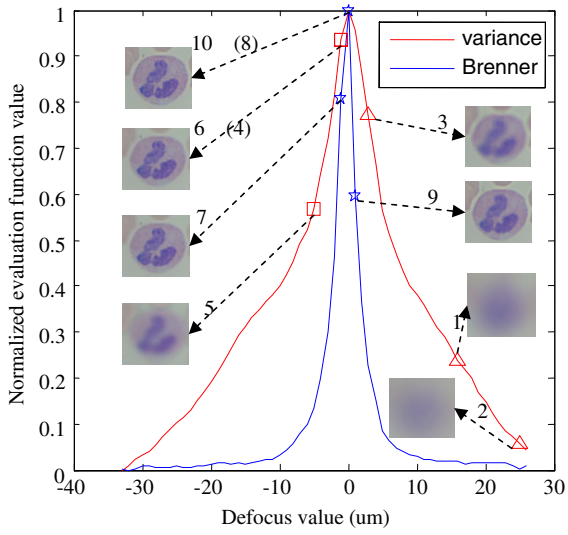

Fig. 13. The auto-focusing process at the beginning position of positive defocus far from the focal plane.

mountaintop. So by leaving the track 1–10, the accurate auto-focusing has come true. Secondly, the beginning position is far from the focal plane with negative defocus. Figure 11 shows one of the experimental results under this circumstance. The beginning position is −27 um far from the focal plane. So the current $F_{\text{var}}(I_0)$ is smaller than 61.6, which means that it may nearly be fallen into the region with many local maximums, while the $step_1$ is 26 um bigger enough adaptively. By taking only a step with $step_1$, it also climbs up the halfway of the mountain at −1 um near the focal plane position and then takes the next steps similar to those in Fig. 10. Thirdly, the beginning position is near the focal plane with positive defocus. Figure 12 shows one of the experimental results under this circumstance. The beginning position is 6 um near the focal plane and is definitely up the halfway of the mountain, while the$F_{\text{var}}(I_0)$ is larger than 241 and the $step_1$ is 7 um smaller enough accordingly. But by taking a step with $step_1$, it will be more and more far away from the mountaintop at 13 um, which means the current searching direction is downhill, so the climbing direction should be changed backward, and the next rough and real mountaintop searching starts at the beginning position to fulfill the accurate auto-focusing. Fourthly, the beginning position is far from the focal plane with positive defocus. Figure 13 shows one of the experimental results under this circumstance. The beginning position is 16 um far from the focal plane, the $step_1$ is as big as 13 um because $F_{\text{var}}(I_0)$ is as small as 123.08. By taking a step with $step_1$, the current position has been fallen in the region with some local maximums and may be nearly out of the focusing range, by taking an additional step with double $step_1$ along the climbing direction, the current position has been up the halfway of the mountain to skip the local maximums. Then after the rough and real mountaintop searching, it can also guarantee efficient auto-focusing.

The above experimental results for auto-focusing have shown its feasibility of the proposed "three steps" MCS algorithm.

In order to analyze the real-time performance of the proposed algorithm, time consumption data are compared and recorded between the original MCS algorithm and the proposed MCS algorithm for different leukocyte images auto-focusing. Table 2 shows the time consumption for 10 different Bas images auto-focusing. The time consumption is shorter within 1690–2100 ms by the proposed algorithm but

Table 2. Time consumption of auto-focusing for Bas (ms).

Test serial	1	2	3	4	5	6	7	8	9	10	$\bar{T}$
MCS algorithm	3893	4052	3540	3722	3524	3919	3583	3364	3751	3371	3672
Proposed algorithm	1944	1921	1930	2109	2016	2338	1947	1935	2104	1693	1994

Table 3. Time consumption of auto-focusing for Eos (ms).

Test serial	1	2	3	4	5	6	7	8	9	10	$\bar{T}$
MCS algorithm	3656	2693	2980	3899	3005	2779	3810	2821	2645	3810	3210
Proposed algorithm	1861	1495	1469	1682	1286	1262	1472	1293	1263	1442	1453

longer within 3524–4052 ms by the original MCS algorithm. Statistically, the time consumption by the proposed algorithm is 1678 ms shorter than that by the original MCS algorithm for their average time ($\bar{T}$). Table 3 shows the time consumption for 10 different Eos images auto-focusing. Though the time consumption for Eos is a little bit shorter than that for Bas as a whole, the $\bar{T}$ by the proposed algorithm is still 1757 ms shorter than that by the original MCS algorithm. So the proposed algorithm can meet the real-time requirement in the blood smear detection.

In order to verify its validity, the proposed algorithm is applied in the blood smear detection including leukocyte images auto-scanning, auto-capturing and auto-extracting. Because the distribution of leukocyte is sparse in a blood smear, few of leukocyte images can be captured in one view field of the CCD camera. Only auto-scanning can obtain the sufficient numbers of different leukocyte images at different regions for effective disease diagnosis. But different defocus values may exist in different scanned regions caused by mechanical errors and motion errors of the object stage, so auto-focusing with the proposed method should be done before image capturing if needed to guarantee the clearness of each captured image in the auto-capturing processing. Because each ROI leukocyte image occupies a small area in each captured full view field image, by auto-extracting processing, each ROI leukocyte image can be figured out and recombined. Thousands of blood smear samples have been detected in this way and the sufficient numbers of clear leukocyte images can be guaranteed for each blood smear sample. Figure 14 shows one of the blood smear detection results. A total of 100 ROI leukocyte images have been extracted and recombined and ROI leukocyte image is realistically clear. The total consumption time is less than 2 min, which means that the proposed improved MCS algorithm is applicable to guarantee sufficient realistically clear leukocyte images and improve blood smear detection efficiency.

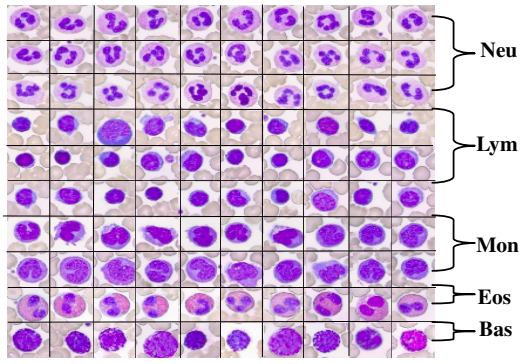

Fig. 14. Extracted ROI leukocyte images scanned in a blood smear.

5. Conclusion

An improved "three steps" MCS algorithm is proposed in which a self-adaptive step length is successfully used to improve the climbing search efficiency and avoid falling into local maximums; by rough and real mountaintop searching, it can reach the mountaintop precisely and as fast as possible. The experimental results show its feasibility and the real-time performance. The proposed algorithm has been applied to the leukocyte blood smear detection successfully to get enough clear leukocyte images for the doctor to diagnose the disease effectively.

Acknowledgment

This work is supported by 863 National Plan Foundation of China under grant No. 2007 AA01Z333.

References

1. X. Liu, M. Yu, Y. Wang, G. Jiang, S. Fu, T. Luo, "A novel time-domain focusing method for microscope imaging," *Procedia Eng.* **15**, 2660–2664 (2011).
2. T. Obara, Y. Igarashi, K. Hashimoto, "Fast and adaptive auto-focusing algorithm for microscopic cell observation," *2011 IEEE/RSJ Int. Conf. Intelligent Robots and Systems*, San Francisco, CA, USA, pp. 7–12 (2011).
3. H. Shi, Y. Shi, X. Li, "Study on auto-focus methods of optical microscope," *The 2012 2nd Int. Conf. Circuits, System and Simulation (ICSS 2012) IPCSIT*, Vol. 46 (IACSIT Press, Singapore, 2012).
4. B. S. Luthi, N. Thomas, S. F. Hiid, P. Rueffer, "An efficient autofocus algorithm for a visible microscope on a Mars lander," *Planet. Space Sci.* **58**, 1258 (2010).
5. A. Santos, C. Ortiz de Solorzano, J. J. Vaquero, J. M. Pena, N. Malpica, F. Del Pozo, "Evaluation of autofocus functions in molecular cytogenetic analysis," *J. Microsc.* **188**, 264 (1997).
6. L. Hui, F. Chengyu, "An improved focusing algorithm based on image definition evaluation," *2011 2nd Int. Conf. IEEE Org. Artificial Intelligence, Management Science and Electronic Commerce (AIMSEC)*, pp. 3743–3746, 8–10 August 2011.
7. K.-S. Choi, J.-S. Lee, S.-J. Ko, "New autofocusing technique using the frequency selection weighted median filter," *IEEE Trans. Consum. Electron.* **45**(3), 820–827 (1999).
8. J. H. Lee, K. S. Kim, B. D. Nam, "Implementation of a passive automatic focusing algorithm for digital still camera," *IEEE Trans. Consum. Electron.* **41**(3), 449–454 (1995).
9. M. Shuxiao, J. Wei, "An improved algorithm for RGB colored images auto-focusing," *IEEE 13th Int. Conf. Communication Technology*, pp. 377–380 (2011).
10. F. C. A. Groen, I. T. Young, G. Ligthart, "A comparison of different focus functions for use in autofocus algorithms," *Cytometry* **6**(2), 81–91 (1985).
11. J. L. Pacheco, G. Cristobal, "Diatom auto focusing in bright field microscope: A comparative study," *Int. Conf. Pattern Recognition (ICPR'00)*, Barcelona, Spain, pp. 314–317 (2000).
12. H. Ramoser, V. Laurain, H. Bischof, R. Ecker, "Leukocyte segmentation and classification in blood-smear images," *Proceeding of the 2005 IEEE, Engineering in Medicine and Biology 27th Annual Conf.*, Shanghai, China, pp. 3371–3374, 1–4 September 2005.
13. K. Ooi *et al.* "An advanced autofocus system for video camera using quasi condition reasoning", *IEEE Trans. Consum. Electron.* **36**(3), 526–530 (1990).
14. L. He, R.-Z. Zhou, Z.-L. Hong, "Modified fast climbing search auto-focus algorithm with adaptive step size searching technique for digital camera," *IEEE Trans. Consum. Electron.* **49**, 257–262 (2003).
15. Y. Song, M. Li, L. Sun, "A new auto-focusing algorithm for optical microscope based automated system," *The 9th Int. Conf. Control, Automation, Robotics and Vision*, Singapore, pp. 1117–1121 (2006).
16. X. Liqun, Y. Zi, W. Jianping, Y. Xinxin, Y. Feihong, "Microscope auto-focusing system with the self-adaptive mountain-climbing search method based on PC control," *Conf. Optical Design and Testing III, Proc. SPIE*, Vol. 6834, Beijing, China, pp. 68342E-1–8 (2007).
17. D. Huang, K. Huang, Y. Chan, "A computer assisted method for leukocyte nucleus segmentation and recognition in blood smear images," *J. Syst. Softw.* **85**, 2104–2118 (2012).
18. Y.-P. Yang, Y.-P. Cao, W.-X. Shi, "A method of leukocyte segmentation based on S component and B component images," *J. Innov. Opt. Health Sci.* **7**(1), 1–8 (2014).